MOLECULAR AND CELLULAR BIOLOGY, Mar. 2001, p. 2144–2153 Vol. 21, No. 6
0270-7306/01/$04.00+0 DOI: 10.1128/MCB.21.6.2144–2153.2001

Dual Inactivation of RB and p53 Pathways in RAS-Induced Melanomas

NABEEL BARDEESY,[1] BORIS C. BASTIAN,[2,3] ARAM HEZEL,[1] DAN PINKEL,[3] RONALD A. DEPINHO,[1,4] AND LYNDA CHIN[1,5]*

Department of Adult Oncology, Dana-Farber Cancer Institute,[1] Department of Medicine and Genetics,[4] and Department of Dermatology,[5] Harvard Medical School, Boston, Massachusetts, and Departments of Dermatology and Pathology,[2] and Comprehensive Cancer Center,[3] University of California, San Francisco, California

Received 26 June 2000/Accepted 14 November 2000

The frequent loss of both INK4a and ARF in melanoma raises the question of which INK4a-ARF gene product functions to suppress melanoma genesis in vivo. Moreover, the high incidence of INK4a-ARF inactivation in transformed melanocytes, along with the lack of p53 mutation, implies a cell type-specific role for INK4a-ARF that may not be complemented by other lesions of the RB and p53 pathways. A mouse model of cutaneous melanoma has been generated previously through the combined effects of *INK4a*$^{\Delta 2/3}$ deficiency (null for *INK4a* and *ARF*) and melanocyte-specific expression of activated RAS (tyrosinase-driven H-RAS^{V12G}, Tyr-RAS). In this study, we made use of this Tyr-RAS allele to determine whether activated RAS can cooperate with *p53* loss in melanoma genesis, whether such melanomas are biologically comparable to those arising in *INK4a*$^{\Delta 2/3-/-}$ mice, and whether tumor-associated mutations emerge in the p16^{INK4a}-RB pathway in such melanomas. Here, we report that *p53* inactivation can cooperate with activated RAS to promote the development of cutaneous melanomas that are clinically indistinguishable from those arisen on the *INK4a*$^{\Delta 2/3}$ null background. Genomewide analysis of RAS-induced *p53* mutant melanomas by comparative genomic hybridization and candidate gene surveys revealed alterations of key components governing RB-regulated G_1/S transition, including c-Myc, cyclin D1, cdc25a, and p21^{CIP1}. Consistent with the profile of c-Myc dysregulation, the reintroduction of p16^{INK4a} profoundly reduced the growth of Tyr-RAS *INK4a*$^{\Delta 2/3-/-}$ tumor cells but had no effect on tumor cells derived from Tyr-RAS *p53*$^{-/-}$ melanomas. Together, these data validate a role for *p53* inactivation in melanomagenesis and suggest that both the RB and p53 pathways function to suppress melanocyte transformation in vivo in the mouse.

Melanocyte-specific H-*RAS*^{V12G} (Tyr-RAS) transgene expression in mice homozygous for the *INK4a*$^{\Delta 2/3}$ mutant allele (null for both *INK4a* and *ARF*) generates a melanoma-prone condition (8). Tyr-RAS-induced melanomas arising in *INK4a*$^{\Delta 2/3}$ heterozygotes invariably sustain deletions in the wild-type INK4a allele, and all such deletions cripple both p16^{INK4a} and p19^{ARF} coding sequences (8). Importantly, despite the high incidence of *p53* mutations associated with the development of many different cancers, the *p53* gene remains intact in these murine melanomas, a genetic profile that appears to hold true for human melanomas as well (see below). Indeed, it was the lack of *p53* mutations in these *INK4a-ARF*-deficient melanomas and in spontaneously immortalized *INK4a-ARF*-deficient fibroblasts, coupled with high levels of p19^{ARF} in p53 null cells (40), that suggested a genetic link between *INK4a-ARF* (specifically, p19^{ARF}) and p53 (8, 27). In line with this genetic relationship, a clear biochemical link has been forged between p19^{ARF} (p14^{ARF} in humans) and p53 through the ability of p19^{ARF} to block MDM2-induced degradation of p53 (26, 39, 54, 61). Correspondingly, tumors arising in *p53* mutant mice maintain an intact *INK4a-ARF* locus (27), thus fortifying the view that p19^{ARF}-MDM2-p53 constitutes a tumor suppressor pathway. This concept follows from the paradigm first proposed to explain the reciprocal pattern of *INK4a* and *RB* mutations in human cancers (reviewed in reference 44).

Evidence supporting a tumor suppression role for p19^{ARF} is exceedingly clear in the mouse and derives from the cancer-prone phenotype of an *ARF*-specific knockout (11, 27) and from the antioncogenic effect of p19^{ARF} on Myc and Ela transformation (39). In addition, p19^{ARF} promotes p53-dependent apoptosis in the setting of aberrant cell proliferation brought about by loss of RB function in vivo (39) or by activation of numerous oncoproteins in primary cultured cells (10, 41, 62) and in vivo (11, 48). Evidence for a tumor suppressor role of p14^{ARF} in humans has been mounting but will remain indirect in the absence of germ line ARF-specific mutations in cancer-prone kindreds (50). While the role of p14^{ARF} in human cancer susceptibility remains unclear, the role of p16^{INK4a} as a human tumor suppressor is irrefutable. Most compelling is the presence of germline mutations that compromise p16^{INK4a} but preserve p14^{ARF} function and confer hereditary susceptibility to melanoma and pancreatic adenocarcinoma (44). Curiously, a role of p16^{INK4a} in tumor suppression may not be as prominent in the mouse, since the *ARF*-specific and *INK4a*$^{\Delta 2/3}$ (null for *INK4a* and *ARF*) knockouts show similar phenotypes with respect to cellular immortalization and cancer susceptibility (24, 27, 49). However, a separate line of evidence has raised the possibility that p16^{INK4a} is relevant in some murine cancer types, such as plasmacytoma (60). Together, these species differences imply that while p16^{INK4a} has a critical tumor sup-

* Corresponding author. Mailing address: Department of Adult Oncology, Dana-Farber Cancer Institute, 44 Binney St., Boston, MA 02115. Phone: (617) 632-6091. Fax: (617) 632-6069. E-mail: lynda_chin@dfci.harvard.edu.

pressor function in humans, its role may be less prominent in the mouse, where tumor suppression appears to be dominated by the $p19^{ARF}$-p53 axis.

Mutation or deletion of p53 has been linked to >55% of all human cancers (17); however, the role of p53 in melanoma remains controversial. Mutational analyses by many groups have shown a very low incidence of point mutation or allelic loss of p53 in surgical specimens of primary and metastatic melanomas (2, 7, 32, 38), while others have estimated the incidence of p53 mutation to be 15 to 25% of primary and metastatic samples (1, 51, 59). Moreover, expression analysis by immunohistochemistry has revealed a significantly higher incidence of p53 overexpression, implying stabilizing point mutations, in metastatic melanomas than in primary melanomas (15), suggesting that loss of p53 function promotes disease progression. In contrast, other groups have reported a lack of correlation between p53 overexpression and stages of melanoma development (12, 43). Indeed, Zerp and colleagues had reported a lower frequency of p53 mutation in metastasis compared with primary melanoma lesions, implying that *p53* mutation, although associated with human cutaneous melanoma arising in sun-exposed sites, does not contribute to melanoma pathogenesis and progression (59).

In this report, we sought to validate a role for functional p53 pathway inactivation in the pathogenesis of melanomas. We demonstrated that RAS activation and *p53* loss cooperate to generate melanomas that are clinically indistinguishable from those arising on an *INK4a-ARF* null background. Furthermore, identification of alterations in key components of the RB pathway by comparative genomic hybridization (CGH) and candidate gene surveys supports a role for both the RB and p53 pathways in melanoma suppression in vivo.

MATERIALS AND METHODS

Mouse strains. Tyrosinase enhancer-promoter-driven H-RAS^{V12G} transgenic mice (8) were crossed onto the *p53* mutant background (Jackson Laboratory) and the $INK4a^{\Delta 2/3-/-}$ background (49) and observed for tumor development or apparent ill health. The Tyr-RAS *p53* mutant mice analyzed in this study were of mixed genetic background (~80% C57BL/6, 20% 129Sv) or N_1 generation FVB backcross (50% FVB, 40% C57BL/6). The Tyr-RAS $INK4a^{\Delta 2/3}$ null mice analyzed were of either mixed genetic background (65% C57BL/6, 25% CBA, 10% 129Sv) or N_3 generation FVB backcross (83% FVB). No consistent difference was noted with respect to tumor latency and CGH profiles in either the mixed genetic background or the FVB backcross generation.

Mouse tumor surveillance and characterization. Mice were observed biweekly for development of tumors or appearance of ill health. Premorbid animals or animals with significant tumor burdens were sacrificed, and detailed autopsies were performed. Tumor specimens were fixed in 10% formalin and embedded in paraffin for histological and immunological analysis as previously described (8). In cases in which sufficient specimens were available, primary tumors were adapted to culture to establish derivative cell lines.

Comparative genomic hybridization. DNA was extracted from microdissected tumor tissue from paraffin-embedded tumor blocks by standard methods (4). Reference and test DNAs labeled with Alexa 594 dUTP (Molecular Bioprobes) and fluorescein-12-dUTP (NEN), respectively, were hybridized to normal metaphase chromosome spreads; chromosomes were identified by 4′,6′-diamidino-2-phenylindole (DAPI) counterstaining, and green-red fluorescence intensity profiles were obtained as previously described (4). Regions were called amplified if the tumor/reference ratio of a chromosomal arm exceeded 1.5 or if the ratio elevation involved a sharply demarcated segment of a chromosomal segment. For the amplification involving chromosome 15, both criteria were met, but in tumors that had focused amplifications involving chromosome 2 or 12, the amplified chromosomal segment was too small to yield a ratio of >1.5.

DNA and RNA analysis. DNA was isolated from snap-frozen tumor specimens or from cell lines derived from primary tumors using the Puregene DNA isolation system (Gentra) according to manufacturer's protocol. Loss of heterozygosity (LOH) analysis of the *p53* locus was done by allele-specific PCR using oligonucleotide primers directed against the wild-type and knockout *p53* alleles (22). The wild-type *p53* allele was amplified using primers 5′P53 (5′-ACAGCG TGGTGGTACCTTAT-3′) and 3′P53WT (5′-TATACTCAGAGCCGGCCT-3′), whereas the mutant allele was amplified by using primers 5′P53 and 3′P53KO (5′-CTATCAGGACATAGCGTTGG-3′). PCRs were performed in a 50-μl volume in 1× PCR buffer (Perkin-Elmer) in the presence of 4 μM $MgCl_2$, 0.8 μM deoxynucleoside triphosphate mix, 1.25 U of AmpliTaq DNA polymerase (Perkin-Elmer), 200 ng of 5′P53, 150 ng of 3′P53KO, 75 ng of 3′P53WT, and 250 ng of genomic DNA. Samples were incubated at 94°C for 2 min, followed by 40 cycles of 94°C for 1 min, 62°C for 2 min, and 72°C for 2 min. PCR products were visualized by agarose gel electrophoresis and ethidium bromide staining.

For sequence analysis of the *ARF* coding sequence, total RNA was isolated from cultured melanoma cell lines using the Trizol reagent (Gibco BRL) according to manufacturer's protocol. A 2-μg RNA sample was used as a template in a reverse transcription reaction using Superscript II polymerase (Gibco BRL) primed with oligo(dT). The coding region of the *ARF* cDNA was amplified by PCR using oligonucleotide primers p19-1 (5′-GTCACAGTGAGGCCGCCGC TGAGGGA-3′) and p19-2 (5′-CTCTTGGGATTGGCCGCGAAGTTCCA-3′). The PCR product was subjected to direct DNA sequencing in both directions using the same primers as above.

To measure changes in gene copy number, genomic DNA was isolated from both primary tumor samples and derivative cell lines by the Puregene DNA isolation system (Gentra) according to manufacturer's protocol and analyzed by slot blot analysis. Blots were hybridized with random primed cDNA probes, and signals were quantitated by PhosphorImager analysis (Fuji BAS). DNA quantities were normalized to hybridization signals of at least two control probes in genomic regions without CGH-detected alteration. The ratio of normalized hybridization intensities on tumor DNA relative to diploid control DNA allowed copy number designations. The control probes used included a 400-bp *Bam*HI/*Eco*RI fragment of *mTERT* (16), a 750-bp fragment of c-*Myc* exon 2, a 270-bp *Sal*I/*Sph*I fragment of *cyclin D1*, full-length *ID2* from pID2k (55), and a 560-bp fragment of N-*Myc* exon 3.

Protein analysis. Cell extracts were prepared from early-passage melanoma cell lines by lysis in radioimmunoprecipitation assay (RIPA) buffer in the presence of protease and phosphatase inhibitors. Lysates were sonicated briefly and clarified by centrifugation. All manipulations of the protein extracts were performed at 4°C. Proteins were quantitated by Bradford assay (Bio-Rad). For immunoprecipitation of $p16^{INK4a}$ complexes, 1 mg of cell extract was precleared by incubation with protein A-Sepharose (Sigma) and preimmune serum and then incubated for 1 h in the presence of anti-$p16^{INK4a}$ antibody M-16 (Santa Cruz). Following addition of protein A-Sepharose, extracts were incubated for an additional 3 h. Precipitated complexes were subjected to sodium dodecyl sulfate-polyacrylamide gel electrophoresis and then transferred to polyvinylidene difluoride filters. The blots were probed with either the $p16^{INK4a}$ antibody used for immunoprecipitation or anti-CDK4 antibody C22 (Santa Cruz). For other Western blot analyses, 50 μg of cell lysates was separated by sodium dodecyl sulfate-polyacrylamide gel electrophoresis or by the NuPAGE Bis Tris gel system (Novex) and transferred to polyvinylidene difluoride filters. The antibodies used in this study included the following: for c-Myc, 06-340 (UBI); for $p19^{ARF}$, AEC40 (39); for RB, 14001A (Pharmingen). The following antibodies were from Santa Cruz Biotechnology: for $p16^{INK4a}$, M-156; for $p15^{INK4b}$, M-20; for $p27^{KIP1}$, C-19; for $p21^{CIP1}$, M-19; for Cdc25a, F-6; for cyclin D1, HD-11 and 72-13G; for cyclin D2, M-20; for cyclin D3, C-16; for β-catenin, C-18; for CDK6, C-21.

Production of retroviruses and infection of melanoma cell lines. cDNAs for human $p16^{INK4a}$ and $p27^{KIP1}$ were cloned into the pBABE puro retrovirus vector. The retrovirus vectors were transfected into the 293GPG packaging cell line (37) using the Lipofectamine 2000 reagent (Gibco BRL). Supernatants containing the retrovirus were filtered and applied to the melanoma cell lines in the presence of 4 μg of Polybrene per ml. Transduced cells were selected 24 h postinfection using 2.5 μg of puromycin per ml. Efficiency of selection was monitored by puromycin treatment of nontransduced cells. Following 48 h of selection, the selected cells were assayed for growth rates and colony formation after low-density seeding. Expression of the exogenous proteins was confirmed by Western blot analyses. Proliferation was assessed by seeding 8,000 cells/well in 12-well plates, followed by counting of viable cells in duplicate on consecutive days. For colony formation, 2,000 transduced cells were seeded on 10-cm-diameter dishes. After approximately 2 weeks, colonies were counted following trypan blue staining.

A

p53 Genotype	Cohort Size	Melanomas			# Death or other tumors
		n =	Incidence	Latency	
+/+	9	0	0%	--	1
+/–	17	2	12%	65 wks	2
–/–	27	7	26%	17 wks	20

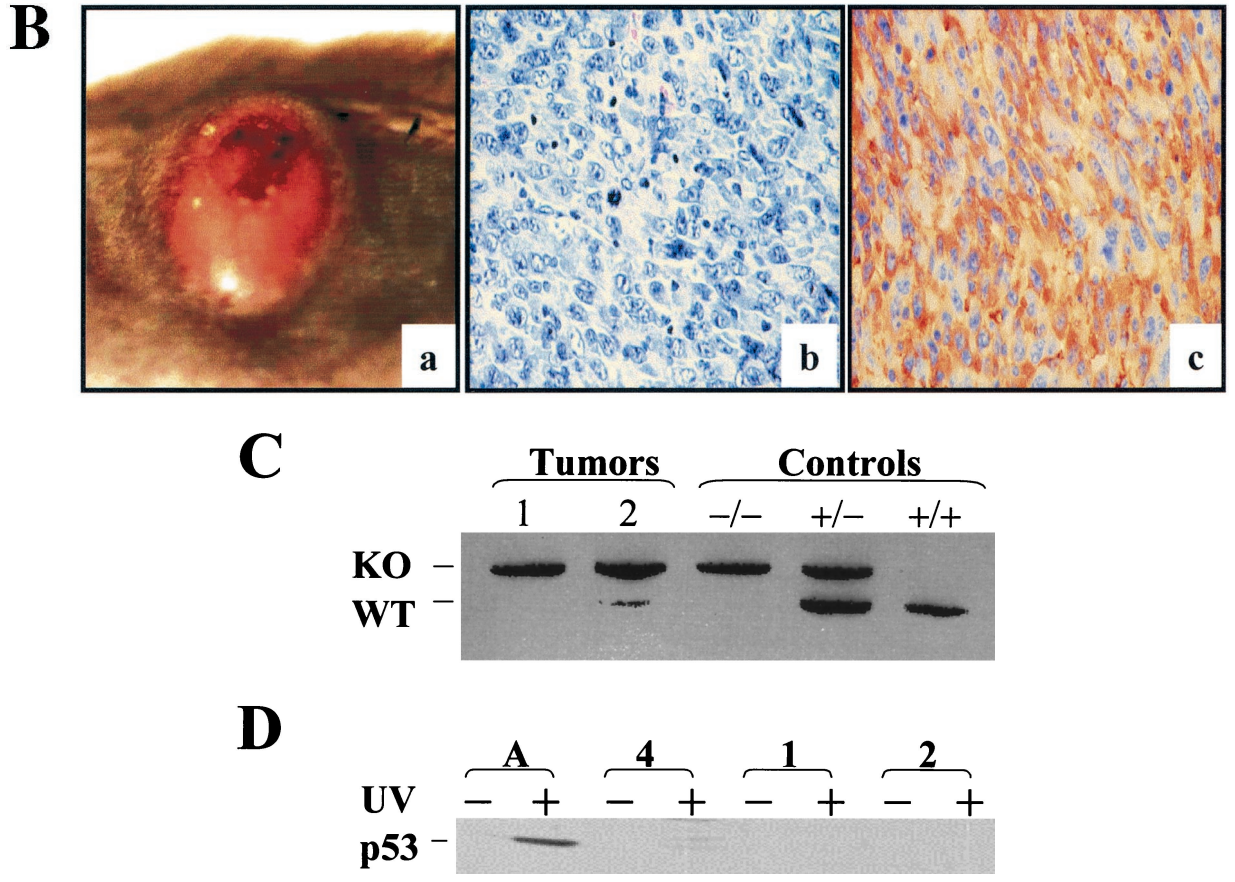

FIG. 1. *p53* deficiency and oncogenic RAS expression cooperate to induce melanoma. (A) Summary of tumor incidence in Tyr-RAS mice in relation to *p53* status. (B) Part a, photograph of a nonpigmented cutaneous melanoma arising on the flank of animal 3. Part b, hematoxylin-and-eosin-stained tumor from animal 3 displaying nuclear pleomorphism and hyperchromasia. Part c, TRP1 immunopositivity demonstrating the melanocytic origin of the tumor. Histology and immunohistochemistry were performed as previously described (8). (C) LOH of *p53* in primary melanoma specimens arising in Tyr-RAS $p53^{+/-}$ mice. DNA was isolated from melanomas arising in Tyr-RAS $p53^{+/-}$ mice (mice 1 and 2) was analyzed by multiplex PCR using primers specific for the wild-type and mutant *p53* alleles. Allelotyping of normal DNA from mice of all three genotypes ($p53^{+/+}$, $p53^{+/-}$, and $p53^{-/-}$) are presented as controls. The bands corresponding to the wild-type (WT) and knockout (KO) *p53* alleles are indicated. (D) Immunoblot analysis of p53 in lysates from tumor cell lines that were either untreated (minus sign) or exposed to UV radiation at 100 J/m^2 (plus sign). Cells were harvested 6 h following irradiation. Tumor A, a melanoma cell line arising in a Tyr-RAS $INK4a^{\Delta 2/3-/-}$ mouse, retains p53 function, while no p53 is induced in melanoma cell lines from Tyr-RAS $p53^{+/-}$ mice (mice 1 and 2). Tumor 4 is derived from a Tyr-RAS $p53^{-/-}$ mouse. (E) Immunoblot analyses of cell lysates from early-passage melanoma cell lines probed with specific antisera show that Tyr-RAS $p53^{-/-}$ melanomas retain expression of $p15^{INK4b}$, $p16^{INK4a}$, and $p19^{ARF}$. (F) Coimmunoprecipitation analysis of melanoma cell lysates using an anti-$p16^{INK4a}$ antibody demonstrates that the $p16^{INK4a}$ expressed in the Tyr-RAS $p53^{-/-}$ melanomas is capable of binding to CDK4. At the top is an immunoblot analysis of melanoma cell lysates probed with antibodies to CDK4 and $p16^{INK4A}$. At the bottom is an immunoblot of complexes immunoprecipitated (IP) with an anti-$p16^{INK4a}$ antibody and probed with antibodies to CDK4 and $p16^{INK4a}$.

RESULTS

Loss of *p53* can cooperate with activated H-RAS^{V12G} to promote melanoma development. In our previous study, over a period of greater than 1 year of observation, only 1 of 49 Tyr-RAS $INK4a^{+/+}$ $p53^{+/+}$ mice developed melanoma that sustained a homozygous deletion of the *INK4a* locus (8). In contrast, Tyr-RAS mice of similar genetic background and harboring mutant *p53* alleles readily developed melanomas, i.e., 2 of 17 Tyr-RAS $p53^{+/-}$ mice and 7 of 27 Tyr-RAS $p53^{-/-}$

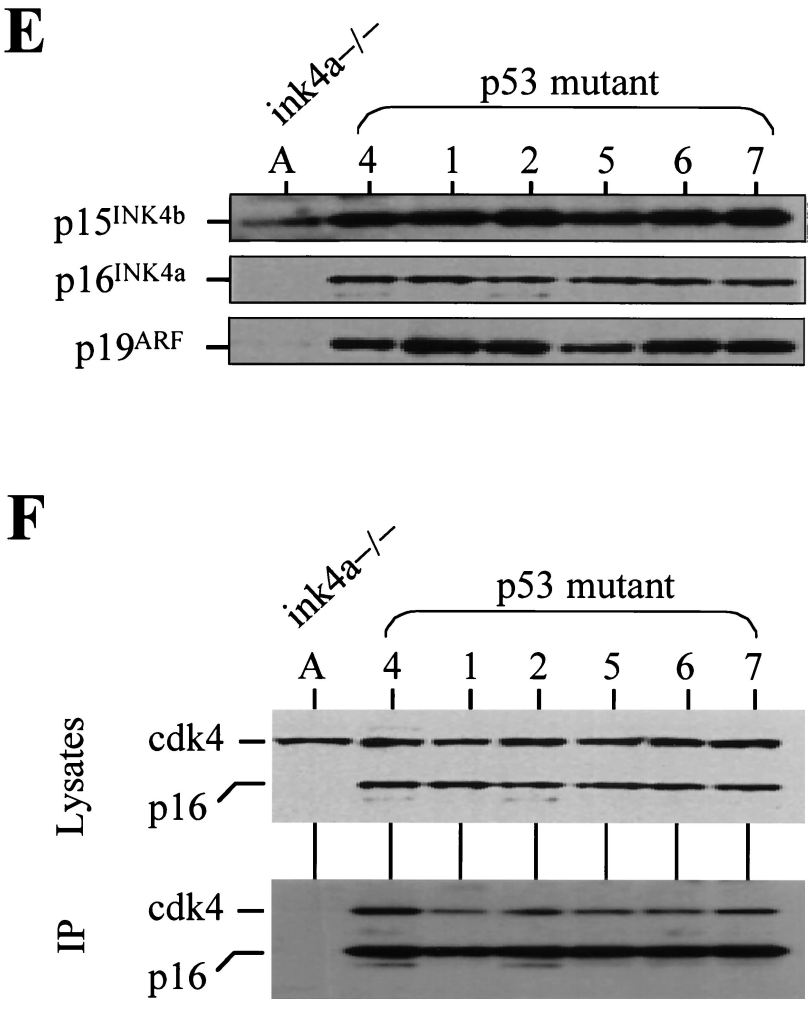

FIG. 1—*Continued.*

mice, with average latencies of 65 and 17 weeks, respectively (Fig. 1A). As expected, additional tumor types (sarcoma and lymphoma) known to be associated with germline *p53* mutation were observed and their early onset (average latency, 17 weeks) likely masked the development of additional melanomas in the *p53*-null cohort.

On the *p53* mutant background, Tyr-RAS transgenic animals developed melanomas that were primarily cutaneous (Fig. 1B, a), with one exception that was ocular in origin (tumor 9). Compared to those arising in Tyr-RAS *INK4a*$^{\Delta 2/3-/-}$ mice, the RAS-induced *p53* mutant melanomas were similarly amelanotic, highly vascular, and locally invasive but not metastatic (8). Microscopically, these dermal tumors were composed of highly pleomorphic, anaplastic cells with characteristic vacuolated nuclei (Fig. 1B, b). The melanocytic origin was confirmed by strong immunoreactivity to the melanocyte-specific marker tyrosinase-related protein 1 (TRP1) (Fig. 1B, c). Together, these data suggest that *p53* mutation can cooperate with activated H-RAS^{V12G} to promote development of nonmetastatic melanomas that are clinically and histologically similar to those observed in Tyr-RAS *INK4a*$^{\Delta 2/3-/-}$ mice.

In the two cutaneous melanomas derived from Tyr-RAS *p53*$^{+/-}$ mice, allele-specific PCR revealed reduction to homozygosity for *p53* (Fig. 1C). That the wild-type *p53* allele was indeed lost was confirmed further by the lack of p53 stabilization following UVB irradiation of early-passage cell lines derived from these primary tumors, in contrast to the intact p53 response to UVB in Tyr-RAS *INK4a*$^{\Delta 2/3-/-}$ tumor cell lines (Fig. 1D). These findings, coupled with the decrease in melanoma latency observed on the *p53*$^{-/-}$ background (Fig. 1A), support a causal role for *p53* loss in the genesis of melanoma in this Tyr-RAS model.

Status of *INK4a-ARF* in melanomas arising in Tyr-RAS *p53* mutant mice. The development of melanoma in *p53* mutant mice provides an opportunity to assess whether loss of *INK4a-ARF*, particularly p16^{INK4a}, is essential for melanomagenesis in mice. In human melanoma, p16^{INK4a} function can be compromised on one of several levels, including deletion or point mutations of the ankyrin repeats of p16^{INK4a} (44), a domain required for interaction with CDK4 and -6 (45), germ line CDK4 mutations that disrupt binding to p16^{INK4a} (57), or cyclin D1 amplifications (20). Here, Western and Southern blot analyses of these mouse melanomas failed to detect gross deletion-rearrangement of *INK4a-ARF* sequences or a de-

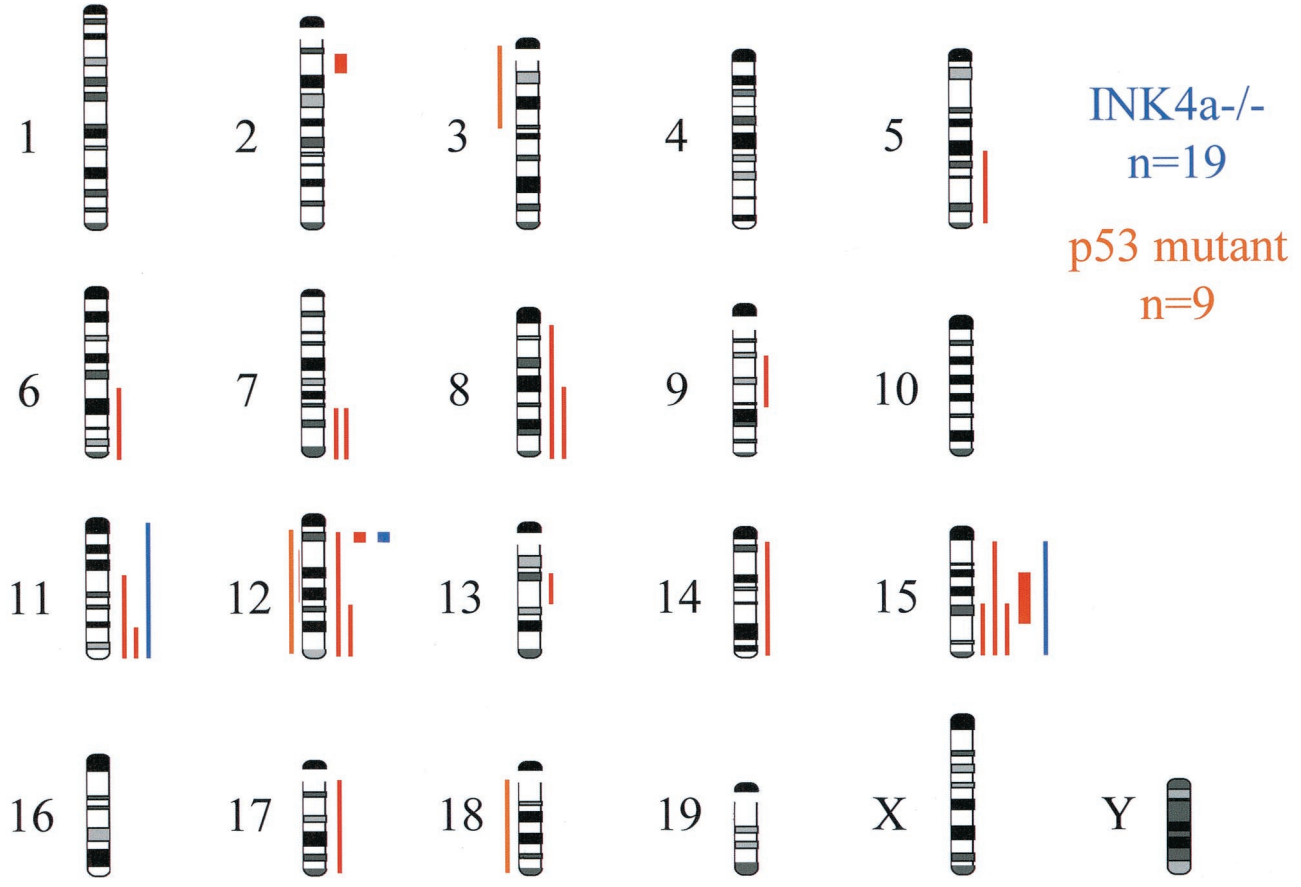

FIG. 2. Chromosomal locations of DNA sequence copy number alterations detected by CGH in RAS-induced melanomas from 9 *p53* mutant mice (red) and 19 *INK4a-ARF* mutant mice (blue). Gains are indicated by lines to the right of the chromosome ideograms, and losses are indicated by lines to the left. Amplifications are indicated by thick lines. A highly amplified focal region at chromosome 12A3 was detected in one Tyr-RAS $p53^{-/-}$ melanoma and one Tyr-RAS $INK4a^{-/-}$ melanoma. The N-*myc* gene is located in the proximity of these amplicons but was present in normal copy number (data not shown).

crease in the levels of all three gene products encoded by this locus: $p15^{INK4b}$, $p16^{INK4a}$, and $p19^{ARF}$ (Fig. 1E; Southern blot not shown). The robust $p19^{ARF}$ expression displayed by the *p53* mutant melanomas is consistent with the loss of a p53-mediated feedback loop in these tumors (27, 54). The functional integrity of the $p16^{INK4a}$ and CDK4 proteins was also substantiated by their mutual coimmunoprecipitation (Fig. 1F). Finally, the $p19^{ARF}$ transcripts from these melanomas were reverse transcription-PCR amplified for direct sequence analysis and found to be free of point mutations (data not shown). Thus, the products of the *INK4a-ARF* locus are expressed and remain structurally intact in melanomas arising in *p53* mutant mice.

Comparative genomic hybridization of RAS-induced melanomas on *INK4a*$^{\Delta 2/3}$ and *p53* mutant backgrounds. The lack of INK4a mutations in Tyr-RAS *p53* mutant melanomas does not exclude the presence of mutations that target other components governing exit from the G_1 phase of the cell cycle. CGH, a technique that permits analysis of the entire tumor genome for alterations in DNA copy number of chromosomal regions (23), was employed as a broad genomic screen to search for tumor-associated changes, particularly those involving loci encoding components that govern the G_1/S transition. A total of 19 Tyr-RAS $INK4a^{\Delta 2/3-/-}$ and 9 Tyr-RAS *p53* mutant melanomas were analyzed (Fig. 2 and Table 1).

The *p53* mutant melanomas possessed a greater degree of chromosomal gains and losses compared with the more euploid profile of the $INK4a^{\Delta 2/3-/-}$ melanomas (2.7 CGH-detected genomic events per tumor versus 0.16 event per tumor, respectively; $P < 0.001$; Fig. 2 and Table 1). The less aneuploid profile of $INK4a^{\Delta 2/3-/-}$, relative to *p53* mutant, melanomas is reminiscent of the benign cytogenetic profiles observed in a murine $ARF^{-/-}$ lymphoma model (48) and in $ARF^{-/-}$ fibroblasts (27). These findings are consistent with the concept that $p19^{ARF}$ is dispensable for p53-dependent control of genomic stability (25).

Overexpression of c-*Myc* in *p53* mutant melanomas. The most common chromosomal abnormality detected by CGH analysis in the *p53* mutant melanomas was gain of chromosome 15 (four of nine mice; Table 1). Collectively, these alterations overlap in the central portion of chromosome 15, a region that encodes the c-Myc oncoprotein, a critical regulator of cellular proliferation (reviewed in reference 9). In dot blot analyses of genomic DNA isolated from primary tumors or their derivative cell lines, hybridization to c-*Myc* confirmed an increase in c-*Myc* gene copy number in these *p53* mutant melanomas (Fig.

TABLE 1. Summary of chromosomal changes detected by CGH in melanomas in relation to *p53* and *INK4a-ARF* genotype[a]

Tumor no.	*p53* status	*INK4a* status	CGH-detected genomic event(s)
1	+/−		enh (6D-G, 7F, 9B-D, 11B-E, 15D3-F), dim (3A-E), amp (2B)
2	+/−		enh (5E-G, 13A5-B), amp (15B3-E)
3	−/−		None
4	−/−		enh (7F, 8C-E, 11C-E, 13A5-B, 14, 15D3-F, 17) dim (12, 18)
5	−/−		None
6	−/−		amp (12A3)
7	−/−		None
8	−/−		enh (12D-F, 15)
9	−/−		enh (8, 12)
A		−/−	None
A2		−/−	None
A3		−/−	None
A4		−/−	enh (15)
A5		−/−	None
A6		−/−	None
A7		−/−	None
A8		−/−	None
A9		−/−	None
A10		−/−	None
A11		−/−	None
A12		−/−	None
A13		−/−	None
A14		−/−	None
A15		−/−	None
A16		−/−	amp (12A3)
A17		−/−	None
A18		−/−	None
A19		−/−	enh (11)

[a] Losses (dim), gains (enh), and amplifications (amp) are indicated (see Materials and Methods).

3B), relative to the signal of two internal control probes (see Materials and Methods). These conventional dot blot assays also revealed one additional tumor (no. 6) whose c-*Myc* gene dosage increase eluded detection by CGH (Fig. 3B), suggesting the presence of more focal gain. These five tumors possessed 1 to 24 extra copies of the c-*Myc* gene, as determined by quantitation of hybridization intensity (Fig. 3B; data not shown). Furthermore, by Western blot analysis, robust c-Myc protein expression can be detected in all six derivative cell lines of Tyr-RAS *p53* mutant melanomas (Fig. 3A and B), at levels that greatly exceed that observed in Tyr-RAS *INK4a*$^{\Delta 2/3-/-}$ samples. The presence of Myc-S, measuring approximately 46 kDa, in tumors 2 and 6 is notable given that this N-terminally truncated c-Myc isoform is oncogenically -competent and often detected in transformed cells (52, 58).

That c-Myc protein expression was found to be elevated in all Tyr-RAS *p53* mutant melanomas, regardless of c-*Myc* gene amplification status, indicates that mechanisms other than increased gene dosage also contribute to deregulated c-Myc expression. Previous cell culture-based studies have demonstrated that high levels of p53 can negatively regulate c-Myc expression (30, 42), raising the possibility that loss of p53-dependent repression accounts for elevated c-Myc expression in Tyr-RAS *p53* mutant tumors. On the other hand, Tyr-RAS *INK4a*$^{\Delta 2/3-/-}$ melanomas display low levels of c-Myc (Fig. 3A) despite having undetectable levels of p53 (Fig. 1D, sample A, and data not shown), arguing against the existence of p53-mediated repression of c-Myc in transformed melanocytes. The up-regulation of c-Myc expression in all of the tumors tested, together with amplification of the c-*Myc* locus in a majority of tumors, is consistent with c-Myc dysregulation being an acquired oncogenic event in *p53* mutant melanomas. These observations gain added significance in light of studies showing that c-Myc can bypass the G_1 block conferred by $p16^{INK4a}$ due, in part, to c-Myc's ability to regulate G_1 molecules operating parallel to and downstream from $p16^{INK4a}$ (reviewed in reference 9). The overexpression of Myc may also contribute to the karyotypic abnormalities detected in the p53 mutant tumors (13).

Alterations in expression of G_1 regulators in *p53* mutant melanomas. Gains in the distal region of chromosome 7 were

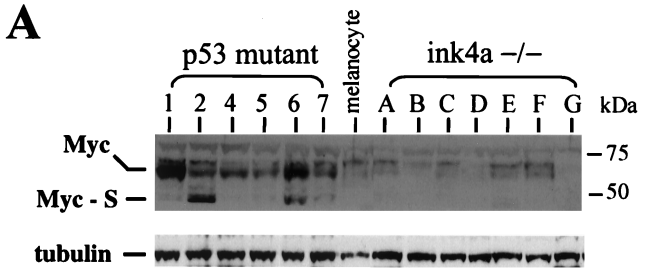

B

Tumor #	c-Myc Locus on Chr 15: Chr Alteration by CGH	c-Myc Locus on Chr 15: Gene Copy # by Dot Blot	c-Myc: Protein Expression
1	enh (15D3-F)	25	High
2	amp (15B3-E)	26	Mod + MycS
3	none	--	--
4	enh (15D3-F)	3	Mod
5	none	2	Mod
6	none	14	Mod + MycS
7	none	2	Mod
8	enh (15)	4	--
9	none	2	--

FIG. 3. Tyr-RAS *p53*$^{-/-}$ melanomas show elevated c-Myc expression and frequent amplification of the c-*Myc* locus. (A) Top, immunoblot showing that c-Myc expression is strongly elevated in *p53* mutant melanoma cells relative to melanocytes (M) and *INK4-ARF* mutant melanomas (A to G). Note the expression of the ~46-kDa short c-Myc isoform (Myc-S) in tumors 2 and 6. The migration of the molecular size markers is indicated to the right. Bottom, immunoblot showing expression of tubulin as a loading control. (B) Summary of genomic alterations at the c-*Myc* locus in *p53* mutant melanomas. Hybridization analysis of melanoma DNA using c-*Myc* and control probes was used to determine the c-*Myc* gene copy number (see Materials and Methods). Note that tumor 6 harbored an amplification of c-*Myc* which was not detected by CGH. c-Myc expression levels (see panel A) are summarized in the rightmost column (Mod, moderate increase in expression). The expression of Myc-S is also indicated. Chr, chromosome.

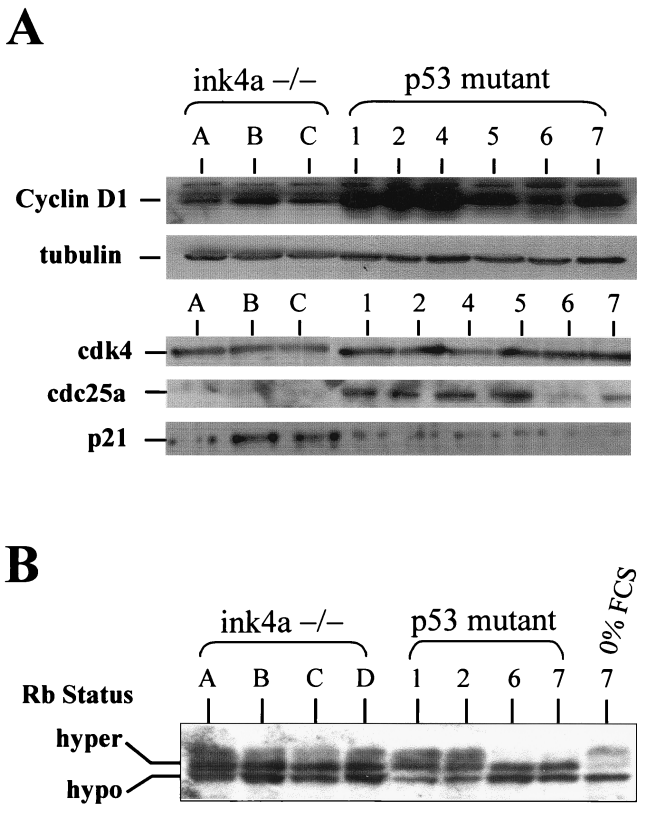

FIG. 4. Expression analysis of G_1/S regulators in RAS-induced melanomas. (A) Top, immunoblot analysis of cyclin D1 levels in melanoma cell lysates from *INK4a-ARF*$^{-/-}$ and *p53*$^{-/-}$ tumors. Below is an immunoblot probed with α-tubulin as a loading control. Bottom, immunoblot of $p21^{CIP1}$, Cdc25a, and CDK4 levels. (B) Western blot analysis of RB phosphorylation status in *INK4a*$^{\Delta 2/3}$-and *p53*-null melanomas. Tumor 7 was grown in 0% fetal calf serum (FCS; rightmost lane) to show that RB is responsive by shifting to a hypophosphorylated state.

detected by CGH in two of nine Tyr-RAS *p53*$^{-/-}$ melanomas examined (Fig. 2). This region encodes cyclin D1, a G_1 cyclin that activates CDK4 and -6 kinase activity that, in turn, phosphorylates and inactivates RB. All *p53* mutant melanomas were shown to express elevated cyclin D1 relative to those present in all of the Tyr-RAS *INK4a*$^{\Delta 2/3-/-}$ melanomas examined (Fig. 4A). Cyclins D2 and D3 were expressed at modest levels in both *INK4a*$^{\Delta 2/3-/-}$ and *p53* mutant samples (data not shown). Given the equivalent levels of CDK4 and CDK6 kinase activity in all of the samples tested (data not shown), it is tempting to speculate that the increased cyclin D1 expression associated with loss of *p53* is a functional equivalent to $p16^{INK4a}$ loss in the Tyr-RAS *INK4a*$^{\Delta 2/3-/-}$ melanomas.

These CGH data prompted expression analysis of factors playing prominent roles in regulating G_1 exit, including $p21^{CIP1}$, $p27^{KIP1}$, and Cdc25a. Levels of the general CDK inhibitor $p21^{CIP1}$ were reduced in the *p53* mutant tumors relative to those in *INK4a*$^{\Delta 2/3-/-}$ melanomas (Fig. 4A). This low level of $p21^{CIP1}$ expression may act to enhance the assembly of active CDK4-D1 complexes (28). The Cdc25a phosphatase, a rate-limiting activator of the CDK2-cyclin E complex, showed higher levels of expression in all *p53* mutant melanomas (Fig. 4A). Since Cdc25a can collaborate with activated RAS to effect cellular transformation and has been reported to be transcriptionally regulated by c-Myc (14, 47), it is possible that enhanced Cdc25a expression reflects elevated c-Myc activity in these *p53* mutant tumors. Alternatively, since the levels of c-Myc and Cdc25a are not tightly correlated in the *p53* mutant tumors, the increased Cdc25a expression may represent an independently acquired event that further facilitates G_1 exit in melanomas with intact $p16^{INK4a}$ function.

RB-mediated G_1/S transition is dysregulated in *p53* mutant melanomas. The finding of c-Myc and cyclin D1 overexpression, coupled with genetic and functional data linking c-Myc to the G_1 cell cycle machinery, suggests that c-Myc and cyclin D1 dysregulation provides an alternative route to RB inactivation, a route that is functionally equivalent to $p16^{INK4a}$ loss in melanoma. Along these lines, the *INK4a*$^{\Delta 2/3}$ -null and *p53* mutant tumors have similar overall RB and E2F activity profiles. Specifically, Western blot analysis showed no differences in RB phosphorylation status between *p53* mutant and *INK4a*$^{\Delta 2/3}$ null melanomas during exponential growth under high- and low-serum conditions or during of confluence (Fig. 4B and data not shown). Correspondingly, E2F transcriptional activity levels assessed by transfection of an E2F reporter construct revealed highly variable, yet overlapping, trends between these *p53* mutant and *INK4a*$^{\Delta 2/3}$ null tumors (data not shown). Together, these data imply that dysregulation of the G_1/S transition—either by $p16^{INK4a}$ loss in an *INK4a*$^{\Delta 2/3}$-null background or by upregulation of c-Myc, cyclin D1, and/or Cdc25a in a *p53* mutant background—is required for melanomagenesis.

To further substantiate that overcoming RB-mediated G_1 arrest is important in the growth of mouse melanomas and to provide evidence that the RAS-induced *p53* mutant melanomas have acquired lesions that bypass this cell cycle block, we assessed the effect of $p16^{INK4a}$ and $p27^{KIP1}$ expression on growth and low-density colony formation in four independently derived *INK4a*$^{\Delta 2/3}$ null and three independently derived *p53* mutant melanoma cell lines. These cell lines were transduced with retroviruses encoding the empty vector, $p16^{INK4a}$, or $p27^{KIP1}$. Levels of protein expression were comparable among the cell lines, as determined by Western blot analysis (data not shown). In RAS-induced *INK4a*$^{\Delta 2/3}$ null melanoma cells, the expression of $p16^{INK4a}$ or $p27^{KIP1}$ strongly inhibited growth and colony formation, relative to those transduced with the empty vector (Fig. 5A and B and data not shown). In contrast, $p16^{INK4a}$ did not substantially affect the growth and colony formation of the RAS-induced *p53* mutant melanoma cell lines, although these cells were was strongly growth inhibited by $p27^{KIP1}$ expression (Fig. 5A and B and data not shown). Given the high levels of c-Myc in the Tyr-RAS *p53* mutant melanoma cell lines, these observations are in accord with several lines of evidence positioning the actions of c-Myc downstream of $p16^{INK4a}$ and at the level of the cyclin E-CDK2 complex (9). It is also possible that these differential responses are dictated, in part, by differences in the levels of Cdc25a and/or $p21^{CIP1}$.

DISCUSSION

In summary, while *p53* deficiency cooperates with oncogenic RAS to confer susceptibility to melanoma development, col-

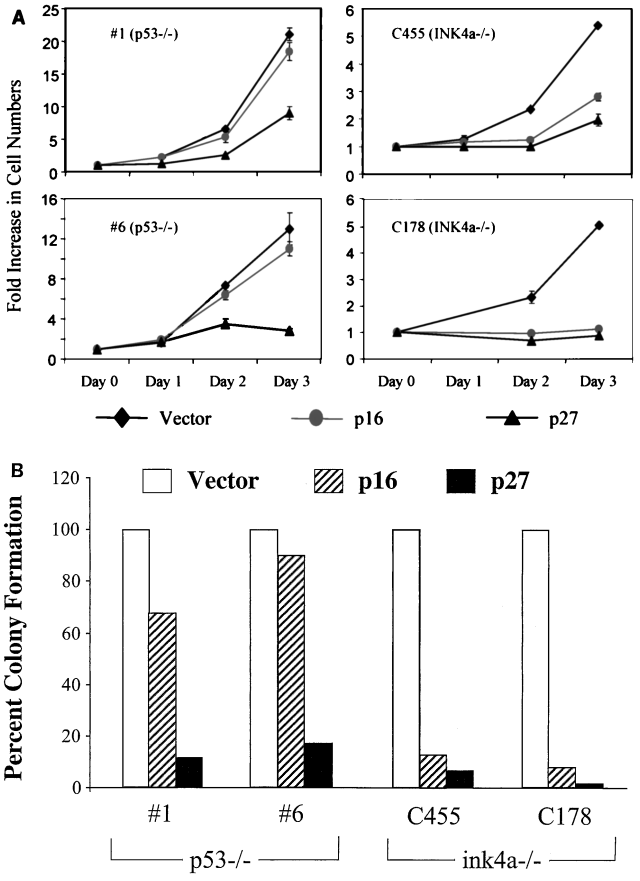

FIG. 5. Effects of exogenous $p16^{INK4a}$ and $p27^{KIP1}$ on the growth of Tyr-RAS melanoma cells on an *INK4a*$^{\Delta 2/3}$-null or *p53* mutant background. (A) Melanoma cell populations transduced with the indicated retroviruses were selected with puromycin for 2 days and then assayed for proliferation rates (see Materials and Methods). Data from two representative cell lines from each genotype are shown. Error bars indicate ranges of variability in duplicate samples assayed. (B) The relative colony-forming ability of the transduced cell lines was determined following low-density seeding (see Materials and Methods). The graph plots the number of colonies as a ratio compared to the number of colonies seen for transduction with the empty vector.

lateral somatic alterations in components known to impinge upon the RB-regulated G_1/S transition are acquired to facilitate G_1 exit. Oncogenic RAS contributes to malignant growth on a number of levels, including alteration of cell motility, cell survival, cell growth, and direct signaling to the G_1 cell cycle machinery (reviewed in reference in 33). With respect to the cell cycle, RAS has been shown to increase assembly of active CDK4-cyclin D complexes. Sustained RAS expression can also induce antiproliferative signals, including up-regulation of $p16^{INK4a}$ and $p21^{CIP1}$ (31). These consequences of RAS activation must be abrogated if a cell is to progress to malignancy. Since the *p53* mutant melanomas sustain alterations in components regulating G_1 exit, it follows that the proliferative signals induced by RAS are insufficient to drive malignant cell proliferation. Indeed, the frequent concurrence of RAS mutations and RB pathway defects in human cancers (34, 46) suggests that the oncogenic actions of RAS extend beyond the regulation of the RB restriction point.

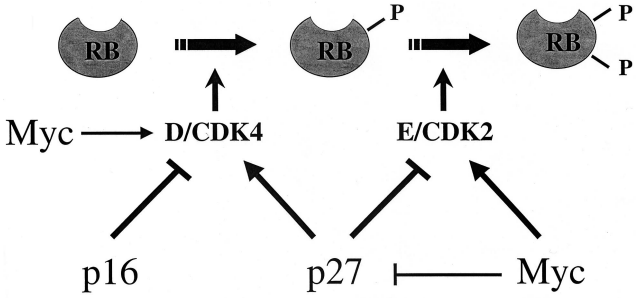

FIG. 6. c-Myc and G_1/S transition. The schematics show sequential phosphorylation of RB during the G_1/S transition. RB phosphorylation is initiated by the activity of CDK4-cyclin D complexes and maintained by that of CDK2-cyclin E complexes. $p16^{INK4a}$ negatively regulates the activity of CDK4, and $p27^{KIP1}$ inhibits the activity of cyclin E-CDK2, although it is also required for assembly of the active CDK4-cyclin D complex. c-Myc can activate the expression of cyclins D1 and D2 (6, 19) and CDK4 (18), leading to type cyclin sequestration of $p27^{KIP1}$ from CDK2 complexes. CDK2 activity is also promoted by the abilities of c-Myc to repress the expression of $p27^{KIP1}$ (29, 56), to downregulate $p27^{KIP1}$ indirectly via upregulation of Cul1 (the SCF complex responsible for its degradation by ubiquitination [36]), and to induce expression of the CDK2 activator Cdc25a (14).

The integral role of c-Myc in driving cellular proliferation is demonstrated by its ability to stimulate S-phase entry and shorten the cell cycle. c-Myc triggers G_1 exit by both promoting an increase in cell mass (21) and modulating expression of genes that control the cell cycle (9). Most of these c-Myc gene targets regulate the activity of G_1 CDKs. c-Myc expression in quiescent cells leads to a rapid induction of cyclin E-CDK2 kinase activity (53), whereas the expression of dominant-negative c-Myc or somatic deletion of c-*Myc* suppresses cyclin E-CDK2 activity (5, 35). c-Myc also activates the expression of cyclins D1 and D2 (6, 19) and CDK4 (18), leading to type D cyclin sequestration of $p27^{KIP1}$ from CDK2 complexes. CDK2 activity is also promoted by the ability of c-Myc to repress the expression of $p27^{KIP1}$ (56) and to induce expression of the CDK2 activator Cdc25a (14). Collectively, these genetic and functional data support a model in which c-Myc stimulates transition through G_1/S (Fig. 6). Expression of either c-Myc or cyclin E allows cells to bypass $p16^{INK4a}$-induced growth arrest, and it is likely that cyclin E-CDK2 is the key functional target of Myc. The resistance of the *p53*-null melanomas to growth inhibition by 16^{INK4a} is consistent with a role for c-Myc in inactivating the RB-mediated restriction point. These results are also analogous to previous studies showing that $p16^{INK4a}$ functions upstream of Myc (3). However, definitive proof that c-*Myc* amplification or overexpression indeed plays a causal role in the genesis of RAS-induced *p53* mutant melanomas requires further genetic studies of the type reported here for *p53* and previously for RAS and *INK4a* (8). The studies described here establish that inactivation of the p53 pathway can play a causal role in the pathogenesis of melanoma. This, coupled with the functional link between $p19^{ARF}$ and p53 and the fact that *INK4a-ARF* loss typically occurs early in the development of human melanomas provides a rational explanation for the rare involvement of direct *p53* mutations in this cancer type—presumably reflecting a diminished need for p53 inactivation in the face of *ARF* loss. Furthermore, the consis-

tent finding of dysregulation of components governing G_1 exit in these *p53* mutant melanomas supports the dual importance of both the RB and p53 pathways in melanoma suppression in vivo. Finally, these results should motivate detailed analyses of c-Myc, cyclin D1, and cdc25a expression in human melanomas harboring *p53* mutations, thereby providing additional targets for rational therapeutic intervention.

ACKNOWLEDGMENTS

We are grateful to Charles Sherr, Martine Roussel, Steven Artandi, Norman Sharpless, Matthew Meyerson, and Kornelia Polyak for critical reading of the manuscript and to Gregory David and Jim DeCaprio for helpful suggestions during the course of this work. We also thank Susan Charzan for excellent technical assistance.

This work was supported by grants from the NIH (K08AR02104-01) and the NCI (U01CA84313-01). N.B. is supported by the American Cancer Society-John Peter Hoffman Postdoctoral Fellowship. B.C.B. was supported by the Marvin and Roma Auerback Melanoma Research Fund. A.H. is an HHMI Medical Student Research Fellow. R.A.D. is an American Cancer Society Research Professor and a Steven and Michele Kirsch Foundation Investigator. L.C. is a V Foundation Scholar. Support from the DFCI Cancer Core grant to R.A.D. and L.C. is acknowledged. D.P., R.A.D., and L.C. are members of the NCI Mouse Models of Human Cancer Consortium.

REFERENCES

1. **Akslen, L. A., S. E. Monstad, B. Larsen, O. Straume, and D. Ogreid.** 1998. Frequent mutations of the p53 gene in cutaneous melanoma of the nodular type. Int. J. Cancer **79:**91–95.
2. **Albino, A. P., M. J. Vidal, N. S. McNutt, C. R. Shea, V. G. Prieto, D. M. Nanus, J. M. Palmer, and N. K. Hayward.** 1994. Mutation and expression of the p53 gene in human malignant melanoma. Melanoma Res. **4:**35–45.
3. **Alevizopoulos, K., J. Vlach, S. Hennecke, and B. Amati.** 1997. Cyclin E and c-Myc promote cell proliferation in the presence of p16INK4a and of hypophosphorylated retinoblastoma family proteins. EMBO J. **16:**5322–5333.
4. **Bastian, B. C., P. E. LeBoit, H. Hamm, E. B. Brocker, and D. Pinkel.** 1998. Chromosomal gains and losses in primary cutaneous melanomas detected by comparative genomic hybridization. Cancer Res. **58:**2170–2175.
5. **Berns, K., E. M. Hijmans, and R. Bernards.** 1997. Repression of c-Myc responsive genes in cycling cells causes G1 arrest through reduction of cyclin E/CDK2 kinase activity. Oncogene **15:**1347–1356.
6. **Bouchard, C., K. Thieke, A. Maier, R. Saffrich, J. Hanley-Hyde, W. Ansorge, S. Reed, P. Sicinski, J. Bartek, and M. Eilers.** 1999. Direct induction of cyclin D2 by Myc contributes to cell cycle progression and sequestration of p27. EMBO J. **18:**5321–5333.
7. **Castresana, J. S., M. P. Rubio, J. J. Vazquez, M. Idoate, A. J. Sober, B. R. Seizinger, and R. L. Barnhill.** 1993. Lack of allelic deletion and point mutation as mechanisms of p53 activation in human malignant melanoma. Int. J. Cancer **55:**562–565.
8. **Chin, L., J. Pomerantz, D. Polsky, M. Jacobson, C. Cohen, C. Cordon-Cardo, J. W. Horner 2nd, and R. A. DePinho.** 1997. Cooperative effects of INK4a and ras in melanoma susceptibility in vivo. Genes Dev. **11:**2822–2834.
9. **Dang, C. V.** 1999. c-Myc target genes involved in cell growth, apoptosis, and metabolism. Mol. Cell. Bio. **19:**1–11.
10. **de Stanchina, E., M. E. McCurrach, F. Zindy, S. Y. Shieh, G. Ferbeyre, A. V. Samuelson, C. Prives, M. F. Roussel, C. J. Sherr, and S. W. Lowe.** 1998. E1A signaling to p53 involves the p19(ARF) tumor suppressor. Genes Dev. **12:** 2434–2442.
11. **Eischen, C. M., J. D. Weber, M. F. Roussel, C. J. Sherr, and J. L. Cleveland.** 1999. Disruption of the ARF-Mdm2–p53 tumor suppressor pathway in Myc-induced lymphomagenesis. Genes Dev. **13:**2658–2669.
12. **Essner, R., C. T. Kuo, H. Wang, D. R. Wen, R. R. Turner, T. Nguyen, and D. S. Hoon.** 1998. Prognostic implications of p53 overexpression in cutaneous melanoma from sun-exposed and nonexposed sites. Cancer **82:**309–316.
13. **Felsher, D. W., and J. M. Bishop.** 1999. Transient excess of MYC activity can elicit genomic instability and tumorigenesis. Proc. Natl. Acad. Sci. USA **96:**3940–4.
14. **Galaktionov, K., X. Chen, and D. Beach.** 1996. Cdc25 cell-cycle phosphatase as a target of c-myc. Nature **382:**511–517.
15. **Grant, S. W., A. S. Kyshtoobayeva, T. Kurosaki, J. Jakowatz, and J. P. Fruehauf.** 1998. Mutant p53 correlates with reduced expression of thrombospondin-1, increased angiogenesis, and metastatic progression in melanoma. Cancer Detect. Prev. **22:**185–194.
16. **Greenberg, R. A., R. C. Allsopp, L. Chin, G. B. Morin, and R. A. DePinho.** 1998. Expression of mouse telomerase reverse transcriptase during development, differentiation and proliferation. Oncogene **16:**1723–1730.
17. **Greenblatt, M. S., W. P. Bennett, M. Hollstein, and C. C. Harris.** 1994. Mutations in the p53 tumor suppressor gene: clues to cancer etiology and molecular pathogenesis. Cancer Res. **54:**4855–4878.
18. **Hermeking, H., C. Rago, M. Schuhmacher, Q. Li, J. F. Barrett, A. J. Obaya, B. C. O'Connell, M. K. Mateyak, W. Tam, F. Kohlhuber, C. V. Dang, J. M. Sedivy, D. Eick, B. Vogelstein, and K. W. Kinzler.** 2000. Identification of CDK4 as a target of c-MYC. Proc. Natl. Acad. Sci. USA **97:**2229–2234.
19. **Hoang, A. T., K. J. Cohen, J. F. Barrett, D. A. Bergstrom, and C. V. Dang.** 1994. Participation of cyclin A in Myc-induced apoptosis. Proc. Natl. Acad. Sci. USA **91:**6875–6879.
20. **Hosokawa, Y., and A. Arnold.** 1996. Cyclin D1/PRAD1 as a central target in oncogenesis. J. Lab. Clin. Med. **127:**246–252.
21. **Iritani, B. M., and R. N. Eisenman.** 1999. c-Myc enhances protein synthesis and cell size during B lymphocyte development. Proc. Natl. Acad. Sci. USA **96:**13180–13185.
22. **Jacks, T., L. Remington, B. O. Williams, E. M. Schmitt, S. Halachmi, R. T. Bronson, and R. A. Weinberg.** 1994. Tumor spectrum analysis in p53-mutant mice. Curr. Biol. **4:**1–7.
23. **Kallioniemi, A., O. P. Kallioniemi, D. Sudar, D. Rutovitz, J. W. Gray, F. Waldman, and D. Pinkel.** 1992. Comparative genomic hybridization for molecular cytogenetic analysis of solid tumors. Science **258:**818–821.
24. **Kamijo, T., S. Bodner, E. van de Kamp, D. H. Randle, and C. J. Sherr.** 1999. Tumor spectrum in ARF-deficient mice. Cancer Res. **59:**2217–2222.
25. **Kamijo, T., E. van de Kamp, M. J. Chong, F. Zindy, J. A. Diehl, C. J. Sherr, and P. J. McKinnon.** 1999. Loss of the ARF tumor suppressor reverses premature replicative arrest but not radiation hypersensitivity arising from disabled atm function. Cancer Res. **59:**2464–2469.
26. **Kamijo, T., J. D. Weber, G. Zambetti, F. Zindy, M. F. Roussel, and C. J. Sherr.** 1998. Functional and physical interactions of the ARF tumor suppressor with p53 and Mdm2. Proc. Natl. Acad. Sci. USA **95:**8292– 8297.
27. **Kamijo, T., F. Zindy, M. F. Roussel, D. E. Quelle, J. R. Downing, R. A. Ashmun, G. Grosveld, and C. J. Sherr.** 1997. Tumor suppression at the mouse INK4a locus mediated by the alternative reading frame product p19ARF. Cell **91:**649–659.
28. **LaBaer, J., M. D. Garrett, L. F. Stevenson, J. M. Slingerland, C. Sandhu, H. S. Chou, A. Fattaey, and E. Harlow.** 1997. New functional activities for the p21 family of CDK inhibitors. Genes Dev. **11:**847–862.
29. **Leone, G., J. DeGregori, R. Sears, L. Jakoi, and J. R. Nevins.** 1997. Myc and Ras collaborate in inducing accumulation of active cyclin E/Cdk2 and E2F. Nature **387:**422–426.
30. **Levy, N., E. Yonish-Rouach, M. Oren, and A. Kimchi.** 1993. Complementation by wild-type p53 of interleukin-6 effects on M1 cells: induction of cell cycle exit and cooperativity with c-*myc* suppression. Mol. cell. Biol. **13:**7942–7952.
31. **Lloyd, A. C.** 1998. Ras versus cyclin-dependent kinase inhibitors. Curr. Opin. Genet. Dev. **8:**43–48.
32. **Lubbe, J., M. Reichel, G. Burg, and P. Kleihues.** 1994. Absence of p53 gene mutations in cutaneous melanoma. J. Investig. Dermatol. **102:**819–821.
33. **Malumbres, M., and A. Pellicer.** 1998. RAS pathways to cell cycle control and cell transformation. Front. Biosci. **3:**887–912.
34. **Mangray, S., and T. C. King.** 1998. Molecular pathobiology of pancreatic adenocarcinoma. Front. Biosci. **3:**1148–1160.
35. **Mateyak, M. K., A. J. Obaya, S. Adachi, and J. M. Sedivy.** 1997. Phenotypes of c-Myc-deficient rat fibroblasts isolated by targeted homologous recombination. Cell Growth Differ. **8:**1039–1048.
36. **O'Hagan, R. C., M. Ohh, G. David, I. M. de Alboran, F. W. Alt, W. G. Kaelin, Jr., and R. A. DePinho.** 2000. Myc-enhanced expression of Cul1 promotes ubiquitin-dependent proteolysis and cell cycle progression. Genes Dev. **14:** 2185–2191.
37. **Ory, D. S., B. A. Neugeboren, and R. C. Mulligan.** 1996. A stable human-derived packaging cell line for production of high titer retrovirus/vesicular stomatitis virus G pseudotypes. Proc. Natl. Acad. Sci. USA **93:**11400–11406.
38. **Papp, T., M. Jafari, and D. Schiffmann.** 1996. Lack of p53 mutations and loss of heterozygosity in non-cultured human melanocytic lesions. J. Cancer Res. Clin. Oncol. **122:**541–548.
39. **Pomerantz, J., N. Schreiber-Agus, N. J. Liegeois, A. Silverman, L. Alland, L. Chin, J. Potes, I. Orlow, H. W. Lee, C. Cordon-Cardo, and R. A. DePinho.** 1998. The INK4a tumor suppressor gene product, $p19^{ARF}$, interacts with MDM2 and neutralizes MDM2's inhibition of p53. Cell **92:**713–723.
40. **Quelle, D. E., F. Zindy, R. A. Ashmun, and C. J. Sherr.** 1995. Alternative reading frames of the INK4a tumor suppressor gene encode two unrelated proteins capable of inducing cell cycle arrest. Cell **83:**993–1000.
41. **Radfar, A., I. Unnikrishnan, H. W. Lee, and R. A. DePinho.** 1998. p19(Arf) induces p53-dependent apoptosis during Abelson virus-mediated pre-B cell transformation. Proc. Natl. Acad. Sci. USA **95:**13194–13199.
42. **Ragimov, N., A. Krauskopf, N. Navot, V. Rotter, M. Oren, and Y. Aloni.** 1993. Wild-type but not mutant p53 can repress transcription initiation in vitro by interfering with the binding of basal transcription factors to the TATA motif. Oncogene **8:**1183–1193.
43. **Rhim, K. J., S. I. Hong, W. S. Hong, S. Y. Lee, D. S. Lee, and J. J. Jang.** 1994. Aberrant expression of p53 gene product in malignant melanoma. J. Korean Med. Sci. **9:**376–381.

44. **Ruas, M., and G. Peters.** 1998. The p16INK4a/CDKN2A tumor suppressor and its relatives. Biochim. Biophy. Acta **1378:**115–77.
45. **Russo, A. A., L. Tong, J. O. Lee, P. D. Jeffrey, and N. P. Pavletich.** 1998. Structural basis for inhibition of the cyclin-dependent kinase Cdk6 by the tumor suppressor p16INK4a. Nature **395:**237–243.
46. **Salgia, R., and A. T. Skarin.** 1998. Molecular abnormalities in lung cancer. J. Clin. Oncol. **16:**1207–1217.
47. **Santoni-Rugiu, E., J. Falck, N. Mailand, J. Bartek, and J. Lukas.** 2000. Involvement of Myc activity in a G1/S-promoting mechanism parallel to the pRb/E2F pathway. Mol. Cell. Biol. **20:**3497–3509.
48. **Schmitt, C. A., M. E. McCurrach, E. de Stanchina, R. R. Wallace-Brodeur, and S. W. Lowe.** 1999. INK4a/ARF mutations accelerate lymphomagenesis and promote chemoresistance by disabling p53. Genes Dev. **13:**2670–2677.
49. **Serrano, M., H. Lee, L. Chin, C. Cordon-Cardo, D. Beach, and R. A. DePinho.** 1996. Role of the INK4a locus in tumor suppression and cell mortality. Cell **85:**27–37.
50. **Sharpless, N. E., and R. A. DePinho.** 1999. The INK4A/ARF locus and its two gene products. Curr. Opin. Genet. Dev. **9:**22–30.
51. **Sparrow, L. E., R. Soong, H. J. Dawkins, B. J. Iacopetta, and P. J. Heenan.** 1995. p53 gene mutation and expression in naevi and melanomas. Melanoma Res. **5:**93–100.
52. **Spotts, G. D., S. V. Patel, Q. Xiao, and S. R. Hann.** 1997. Identification of downstream-initiated c-Myc proteins which are dominant-negative inhibitors of transactivation by full-length c-Myc proteins. Mol. Cell. Biol. **17:**1459–1468.
53. **Steiner, P., A. Philipp, J. Lukas, D. Godden-Kent, M. Pagano, S. Mittnacht, J. Bartek, and M. Eilers.** 1995. Identification of a Myc-dependent step during the formation of active G1 cyclin-cdk complexes. EMBO J. **14:**4814–4826.
54. **Stott, F. J., S. Bates, M. C. James, B. B. McConnell, M. Starborg, S. Brookes, I. Palmero, K. Ryan, E. Hara, K. H. Vousden, and G. Peters.** 1998. The alternative product from the human CDKN2A locus, p14(ARF), participates in a regulatory feedback loop with p53 and MDM2. EMBO J. **17:**5001–5014.
55. **Sun, X. H., N. G. Copeland, N. A. Jenkins, and D. Baltimore.** 1991. Id proteins Id1 and Id2 selectively inhibit DNA binding by one class of helix-loop-helix proteins. Mol. Cell. Biol. **11:**5603–5611.
56. **Vlach, J., S. Hennecke, K. Alevizopoulos, D. Conti, and B. Amati.** 1996. Growth arrest by the cyclin-dependent kinase inhibitor p27Kipl is abrogated by c-Myc. EMBO J. **15:**6595–6604.
57. **Wolfel, T., M. Hauer, J. Schneider, M. Serrano, C. Wolfel, E. Klehmann-Hieb, P. E. De, T. Hankeln, z. B. K. H. Meyer, and D. Beach.** 1995. A p16INK4a-insensitive CDK4 mutant targeted by cytolytic T lymphocytes in a human melanoma. Science **269:**1281–1284.
58. **Xiao, Q., G. Claassen, J. Shi, S. Adachi, J. Sedivy, and S. R. Hann.** 1998. Transactivation-defective c-MycS retains the ability to regulate proliferation and apoptosis. Genes Dev. **12:**3803–3808.
59. **Zerp, S. F., A. van Elsas, L. T. Peltenburg, and P. I. Schrier.** 1999. p53 mutations in human cutaneous melanoma correlate with sun exposure but are not always involved in melanomagenesis. Br. J. Cancer **79:**921–926.
60. **Zhang, S., E. S. Ramsay, and B. A. Mock.** 1998. Cdkn2a, the cyclin-dependent kinase inhibitor encoding p16INK4a and p19ARF, is a candidate for the plasmacytoma susceptibility locus, Pctrl. Proc. Natl. Acad. Sci. USA **95:**2429–2434.
61. **Zhang, Y., Y. Xiong, and W. G. Yarbrough.** 1998. ARF promotes MDM2 degradation and stabilizes p53: ARF-INK4a locus deletion impairs both the Rb and p53 tumor suppression pathways. Cell **92:**725–734.
62. **Zindy, F., C. M. Eischen, D. H. Randle, T. Kamijo, J. L. Cleveland, C. J. Sherr, and M. F. Roussel.** 1998. Myc signaling via the ARF tumor suppressor regulates p53-dependent apoptosis and immortalization. Genes Dev. **12:**2424–2433.